Single Molecule Probes

Lori S. Goldner,[*a] Kenneth D. Weston,[a] William F. Heinz,[a] Jeeseong Hwang,[a] Eric S. DeJong,[b]
John P. Marino[b]
[a]Optical Technology Division, NIST, Gaithersburg, MD 20899-8441 USA
[b]Center for Advanced Research in Biotechnology, NIST, Rockville, MD 20850 USA

ABSTRACT

The technology to rapidly manipulate and screen individual molecules lies at the frontier of measurement science, with impacts in bio- and nano-technology. Fundamental biological and chemical processes can now be probed with unprecedented detail, one molecule at a time. These "single molecule probes" are most often fluorescent dye molecules embedded in a material or attached to a target molecule, such as a protein or nucleic acid, whose behavior is under study. The fluorescence from a single dye molecule can be detected, its spectrum and lifetime measured and its absorption or emission dipole calculated. From this information, the rotational and translational dynamics of the fluorophore can be calculated, as can details of its photophysics. To the extent that these properties reflect the properties of the target molecule, we can use these fluorescent tags to probe the dynamics and structure of the target. In this work we discuss the dependence of the physical and photophysical dynamics of fluorescent molecules on their local environment, and we use confocal microscopy to study single molecules in thin films, on surfaces, and in various liquid and gaseous environments.

Keywords: Confocal microscopy, single molecule, fluorescence, RNA, polymers

INTRODUCTION

Measurement of the fluorescence intensity, spectrum, lifetime, alignment, and polarization anisotropy of single molecules *in-situ*, *in-vitro*, and more recently, *in-vivo*, enables the study of heterogeneous and non-equilibrium microenvironments that are obscured in ensemble measurements.[1-4] The fluorescence from single dye molecules has been used to report back on the local chemical and physical environment in polymers,[5-7] sol-gels,[8,9] biological membranes,[10-12] and living cells.[13-15] Single molecule fluorescence has also been used to elucidate the motion of molecular motors,[16-18] follow single enzymatic reactions,[19,20] and monitor the conformational changes of single proteins.[21,22]

All single molecule fluorescence studies make use of a fluorescent probe that is either bound to a larger target molecule, distributed dilutely in a matrix material, or adsorbed on a surface. The target molecule may be, for example, a nucleic acid bound to the surface of a diagnostic chip. In an example given below, a fluorescently tagged RNA is bound to the surface of a glass coverslip. Three questions need be answered before this system can be useful in a single-molecule study. First: To what extent does the addition of a fluorophore modify the behavior of the target? This question is most often addressed using bulk assays that do not require the use of the fluorescent tag. These assays miss details that may be embedded in the distribution or time-dependence of molecular properties. Second: To what extent does the behavior of the fluorophore reflect the properties of the target? This question is more difficult to answer and requires first that we understand how different environments affect the tag, independent of the target. Finally: To what extent does the presence of the surface modify the behavior of this target molecule? This question can only be fully answered at the single molecule level after the first and second questions have been answered.

Here we work primarily towards the answer to the second question. In particular, we discuss the dynamics and photophysics of dye molecules in different gaseous and liquid environments, on surfaces and in solution, and some techniques used to study these dynamics. We discuss how these various physical environments can affect the fluorescence from single molecules. We concentrate on intensity fluctuations and rotational dynamics.

In the first section of this paper we discuss single molecule fluorescence and confocal detection of single molecule fluorescence. The origin of intensity fluctuations in single molecule fluorescence is reviewed and the rotational dynamics of dye molecules on surfaces and in thin films, which affects the polarization and intensity of the fluorescence, is discussed. The second section considers the effect of atmospheric conditions on fluorescence and presents data of single molecule

[*] lori.goldner@nist.gov, NIST Stop 8441, Gaithersburg, MD 20899.

fluorescence in air, oxygen, and nitrogen gas. Finally we discuss the intensity fluctuations and rotational dynamics of single dye molecules on surfaces and in aqueous solution, including dye-tagged RNA molecules bound to a surface.

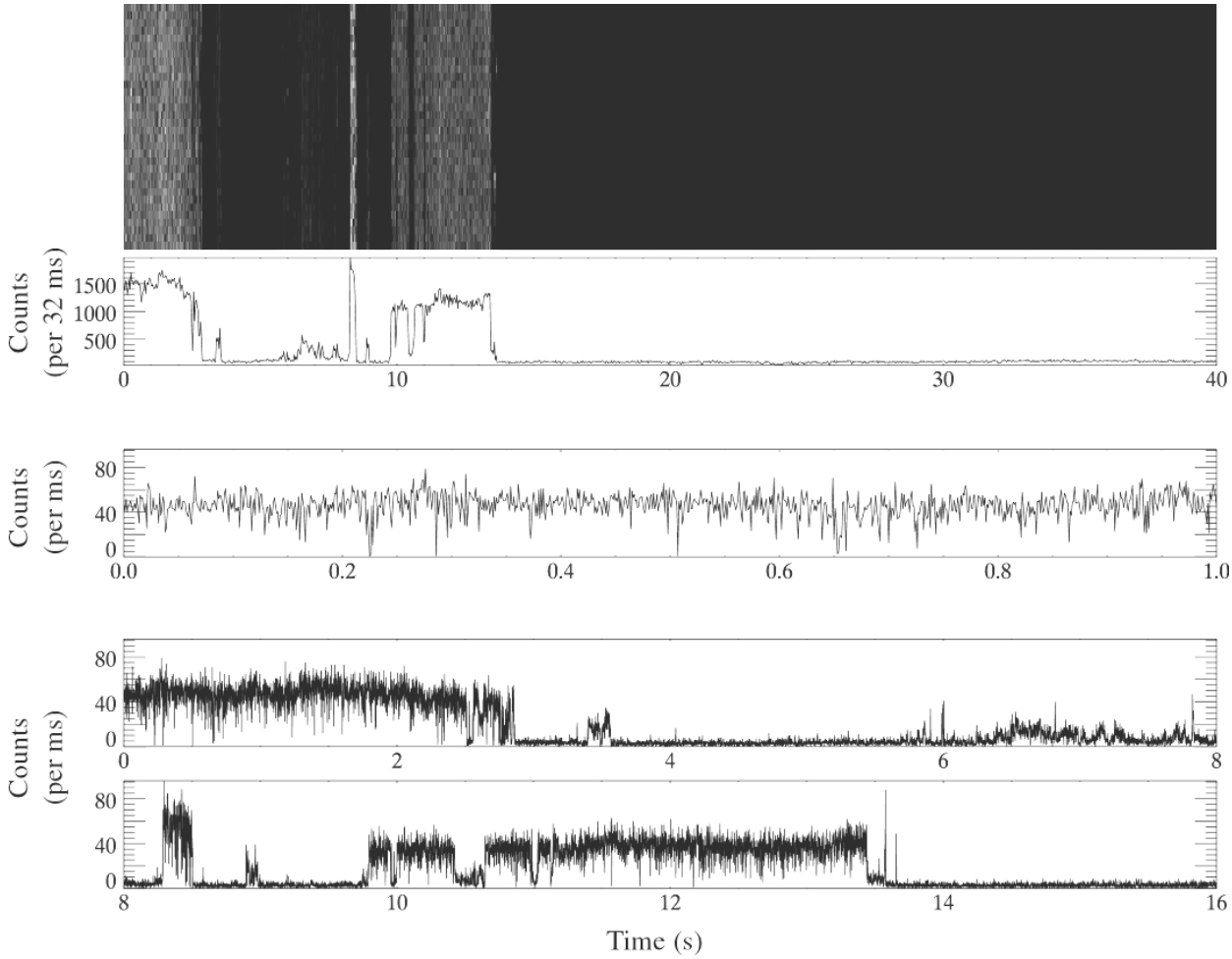

Figure 1. The fluorescence intensity trajectory from a typical $DiIC_{18}$ molecule under ambient conditions. For this sample, the dye molecules are embedded in a 60 nm thick polystyrene (PS) film made by spin casting 10 μL of a 1 mg/mL polymer, 0.1 nmol/L dye solution in chloroform onto a pre-cleaned cover glass substrate. The data set is comprised of intensity measurements in 1 ms bins for a total of 40 s. In the top panel, all of the data are displayed in a grayscale format; each column in the image represents 32 ms (1250 columns). Below the image is plotted the total fluorescent photon counts in every 32 ms interval vs. time. The second plot shows the first 1 s of data plotted on an expanded time scale. The bottom two plots show the first 16 s of data on an expanded time scale.

1. MOLECULES AT SURFACES AND IN THIN FILMS

1.1 Single molecule fluorescence

The fluorescence vs. time from a single $DiIC_{18}$ (1,1'-dioctadecyl-3,3,3',3'- tetramethylindocarbocyanine perchlorate) molecule embedded in a thin polystyrene film is shown in Figure 1. Here fluorescence data are acquired by counting the number of photons arriving at a detector in 1 ms intervals for a total of 40 s. The top panel shows all 40,000 intensity data points, with time on both axes and the number of fluorescent photons represented by the grayscale (0 = black, 92 = white). The vertical axis is 32 ms long, and the very first data point is plotted on the lower left. The second column contains the next 32 data points, beginning at the bottom, and so on. Below the grayscale image we plot the total number of photons arriving at the detector in a 32 ms interval vs. time, and below that are plotted all the data in the first 1 second and the first 16 s of the measurement. Several features are evident from this data. First, the molecule emits at several different intensity levels and

switches between these on a slow (1 s) time scale. Second, this molecule undergoes what appears to be irreversible photobleaching before 14 s, although it is possible that this state is merely another dim state. Finally, even within time intervals of the data that appear to have steady intensity, there is intensity noise beyond that expected from shot noise, *i.e.*, the fluctuations are non-Poisson. For example, the photon count rate averaged over the first second, is 46.1 ms^{-1}. The rms value of the noise is 10.9 ms^{-1}. For a shot-noise limited (Poisson) source, this number would be closer to 6.8 ms^{-1}. Furthermore, the fluctuations are not symmetric about the mean; they are predominantly towards a smaller number of photons, and in several places go to zero. In an ensemble measurement, these features would not be evident. We would measure a constant fluorescence intensity that may decay slowly over time due to photobleaching, and the measurement would likely be shot-noise limited. From this we might assume that an "average molecule" would simply look like a dimmer version of the ensemble. From bulk measurements we have no evidence for the remarkable time dependence in the fluorescence intensity of a single molecule that is demonstrated in Figure 1.

The changes in fluorescence intensity are, in part, caused by the environment of the molecule. In general, a dye molecule has an energy-level scheme (Jablonski diagram) similar to that shown in Figure 2. Here S_0 is the ground electronic state, S_1 is the first singlet excited state, and T_1 is a triplet state. The (power dependent) excitation rate is given by k_{abs}, k_{fl} is the radiative decay rate out of S_1, and $k_{nr}^{S_1}$ is the nonradiative decay rate of S_1. The rate of intersystem crossing into the triplet state is given by k_{isc} and the lifetime of the triplet state is τ_{T_1}. Generally the decay rate of the excited singlet state to the ground state $(k_{fl} + k_{nr}^{S_1})$ is much faster than k_{isc}. When τ_{T_1} is much shorter than the signal integration time, the fluorescence intensity is expected to be shot-noise limited. The fast fluctuations that give rise to the non-Poisson statistics in the first second of the data shown in Figure 1 are evidence that the molecule occasionally resides in the triplet state.[23] This triplet "shelving" is particularly noticeable upon removal of O_2 which normally acts to quench or shorten the triplet lifetime.[24-26] This is discussed in more detail in Section 2. The slower changes between different intensity levels in Figure 1 then correspond to changes in the other rates, which might for example be caused by changes in the spectrum. Changes in spectrum or rate constants might in turn be brought on by conformational changes in the molecule or physical or chemical changes in its environment.[27,28] While not all molecules exhibit the rich behavior of this individual, very few indeed look like the "average" molecule whose properties might be deduced from the properties of the ensemble (even when including photobleaching in our definition of "average").

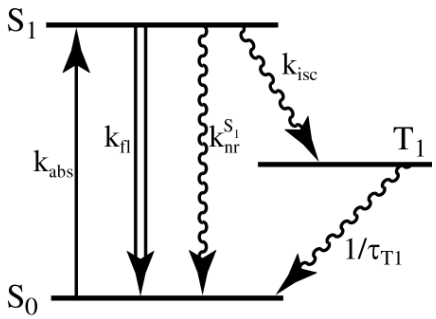

Figure 2. Jablonski Diagram that represents the various states and processes involved in fluorescence phenomena.

1.2 Instrumentation

A schematic of the apparatus, which has been described in a previous publication, [7] is shown in Figure 3a. A linearly polarized CW laser beam at λ=532 nm is passed through an electro-optic modulator (EOM) and quarter-wave plate (QWP). The EOM and waveplates are for the fluorescence polarization modulation experiments described below and were not used for the data taken in Figure 1. Two dielectric mirrors are used to direct the beam through an expander and into the rear port of an inverted microscope (mirrors and beam expander not shown). Data are generally taken with laser input power of about 1 μW. A dichroic beamsplitter (Chroma Technology 545 DCLP) reflects the laser beam that is then focussed (to ≈ 400 nm in diameter, limited by diffraction and the quality of the beam spatial mode) on a cover glass surface using an oil immersion objective (NA of 1.25 or 1.4). This objective is also used to collect laser-induced fluorescence; the red shifted emission passes through the dichroic beamsplitter (>90% transmissivity for λ = 550-720 nm). A holographic notch filter is used at the detector to further reduce background excitation light. The 150 μm diameter active area of a silicon avalanche photodiode (APD) used for photon counting is positioned in the microscope image plane. The use of a confocal detection scheme means that the detection volume in these experiments is always ~ 1 fL. This small volume, and the corresponding rejection of background fluorescence, is what makes the signal-to-noise ratio large enough to permit sensitive single molecule fluorescence intensity measurements. An X-Y stage with piezo-electric actuators scans the sample and is controlled using two digital-to-analog output channels of a computer interface board. The same board counts photon-generated pulses from the APD. The sample can either be positioned directly over a molecule while data are acquired for long periods of time, or the sample can be scanned to form images with single molecule sensitivity.

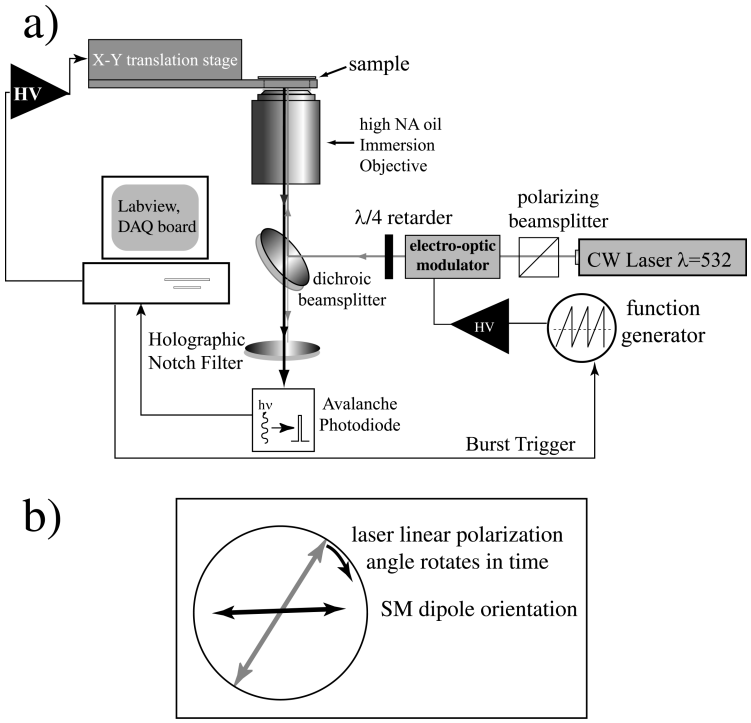

Figure 3. (a) Schematic of the sample scanning confocal microscope with polarization rotation capabilities for our single molecule research. The electro-optic modulator, when driven with a ramp waveform (−190V to +190 V) and in combination with the λ/4 retarder generates linearly polarized laser light which rotates in time. (b) Fluorescence from a molecule with a well defined absorption dipole axis excited with light will be modulated with a phase that depends on the orientation of its absorption dipole.

For the polarization modulation experiments, the EOM (45°) and QWP (vertical=0°) are oriented with respect to the laser polarization (vertical) so that linearly polarized light oriented at an angle proportional to the voltage applied to the EOM is generated. The EOM was driven by a ramp waveform (−190 V to +190 V) through retardance from −λ/2 to λ/2. With the QWP as described above, linearly polarized light with polarization angle rotating in time through 180 degrees is generated. The phase of the modulated fluorescence with respect to that of the ramp waveform used to drive the EOM indicates the orientation of the absorption dipole of the molecule. This imaging technique is conceptually analogous to that reported in Ref. (29) used to spatially resolve absorption dichroism in mesostructured materials. T. Ha *et al.* [30] used polarization modulation to measure the orientation of single molecules on a somewhat slower time scale than that presented here. Orientation imaging of single molecules using this method was demonstrated in a recent work by some of the present authors.[7]

We discuss only orientation in the (X-Y) sample plane and make no attempt to measure orientation in z (the optical axis of the system) in these experiments. Several recent papers discuss techniques for measuring the z-component of the absorption dipole.[31-34]

1.3 The rotational dynamics of single molecules

One cause of intensity fluctuations for the molecules in Figure 1 is rotational motion. The intensity is dependent upon the relative orientation of the excitation polarization and the molecule's absorption dipole moment (which affects k_{abs}). When these are aligned absorption, and thus fluorescence, is maximized. Conversely, when they are perpendicular the absorption is zero and fluorescence near the background level is observed. The rotational mobility of a fluorophore is expected to be dependent on its chemical and physical environment. One might think that molecules adsorbed on a surface or embedded in a polymer below T_g, the glass transition temperature, would not show any rotational dynamics since their interaction with the surface or polymer would presumably hold them in place. Instead, molecules in thin polymer films and on surfaces demonstrate a wide range of orientation dynamics and can be used as sensitive probes of their immediate environment. [6,7]

In general, the ability to 'watch' molecular orientation has significant impact on scientific discovery in biology, chemistry, and physics. A great deal of current research seeks to understand rotational mobility of proteins and lipids in cell membranes and in cellular function. [4,16-20,22,35] Studies of binding and catalysis that use the efficiency of fluorescence resonance energy transfer (FRET) as a proximity probe [4,36,37] can be improved when combined with high precision orientation information, since the FRET efficiency depends on relative orientations of donor and acceptor chromophores. For materials science, single molecule orientation monitoring is attractive for understanding molecular scale motions and site heterogeneity in polymeric and self-assembled systems. One technologically important example is the development of chromophore doped polymers as inexpensive alternatives to inorganic nonlinear optical (NLO) materials.[38] In this case, the temporal decay in alignment of poled chromophores in polymers has prevented widespread application of polymer NLO materials.[39] Another topic of intense research and debate involves understanding how and why polymer properties in thin films differ from bulk properties.[40-43] These research fields can benefit from new insight provided by observing the static and dynamic properties of individual chromophores.

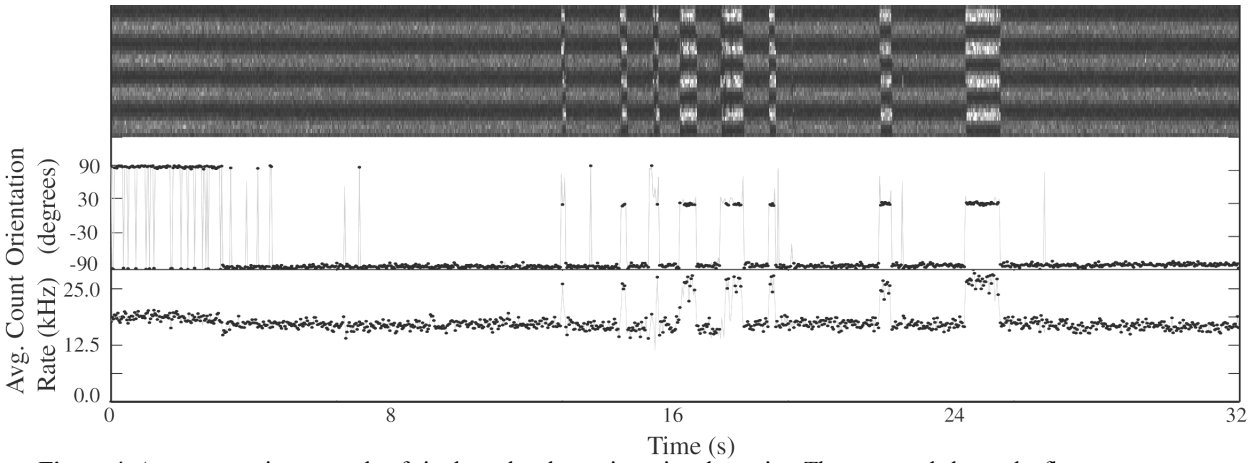

Figure 4. A representative example of single molecule reorientation dynamics. The top panel shows the fluorescence intensity data for a $DiIC_{18}$ molecule in a 60 nm thick PVB film using the same format as in Figure 1. This molecule, however, was excited with rotating linearly polarized light. Each column displays 32 ms and 4 modulation cycles of data. The phase of the modulated fluorescence gives the orientation. Large and instantaneous (on the time scale of our measurement) jumps in orientation are observed. The corresponding orientation and average count rate are also plotted. This molecule visited three different orientations during the measurement.

In a recent report, the orientation of single rhodamine 6G molecules has been tracked for hours and used to study the rotational freedom of motion within poly(methylacrylate) thin films near T_g, the glass transition temperature.[6] In Figure 4 we track the rotational dynamics of a molecule in a polymer at room temperature, well below T_g, with 32 ms resolution. Here the molecule is $DiIC_{18}$ embedded in a poly(vinyl butyral) (PVB) film 60 nm ± 20 nm thick, with molecular weight[44] M_W =115,000 and T_g = 51 °C. The molecule is illuminated with polarization modulated light and the fluorescence is collected, as discussed above. A molecule that is stationary will display maximum fluorescence when the excitation polarization is aligned along the absorption dipole axis of the molecule. The fluorescence will be zero when the excitation light is polarized perpendicular to the absorption dipole. Out-of-plane components of the absorption dipole axis will decrease the maximum fluorescence (decrease k_{abs}) but the minimum in the fluorescence remains zero. Molecules that are completely free to move, and do so on a time scale much faster than the 125 Hz polarization modulation, will have fluorescence that is independent of the phase of the excitation polarization. The top panel of Figure 4 shows the fluorescence of a single molecule over 32 s plotted in the same way as the data of Figure 1. Here the polarization modulation leads to intensity modulations that are evident as stripes in Figure 4 (top), indicating that this molecule is stationary. The phase of these stripes gives the absolute orientation of the molecule; the jumps in position of the stripes are clear evidence for orientation jumps of this molecule. Approximately one-half of the molecules in any given sample show rotational motion on this 32 second time scale. Rotational behavior varies widely from molecule to molecule, with some molecules diffusing quickly around (too fast to be tracked in this experiment) while others show clear "pauses" at preferred positions with fast diffusion in between and some, like the one in Figure 4, with just a few quasi-stable positions, fast jumps between them, and no evidence for diffusion between states. Molecules distributed on bare glass substrates show similar behavior, indicating that the difference

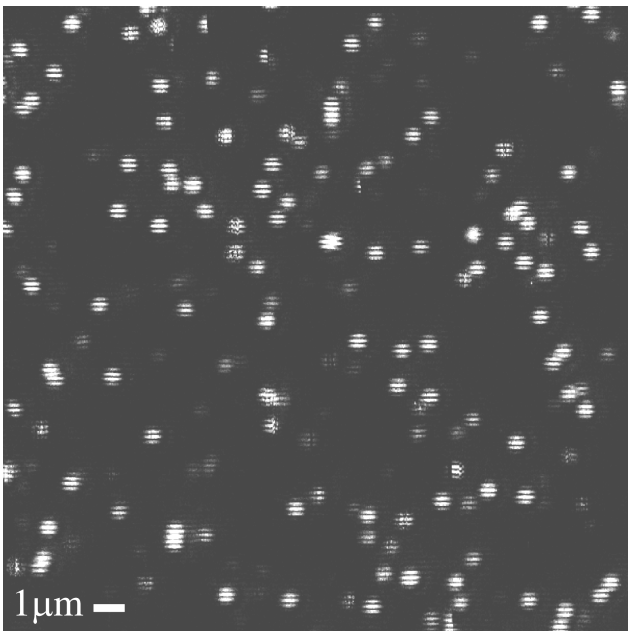

Figure 5. Single $DiIC_{18}$ molecules embedded in a 60 nm thick PVB film. The beginning of each scan line (vertical) is synchronized with the initiation of polarization rotation, resulting in bright and dark stripes indicative of molecular orientation (see text). The image is acquired with polarization modulation frequency of 200 Hz, laser power of 1 μW, and 1ms bin time per pixel. The image is 600 × 600 pixels (20 μm × 20 μm).

in rotational motion is likely due to differences in the static micro-environments of the molecules and not dynamics in the polymer. Subtle differences appear for molecules in different thickness polymer films; in general there is more rotational motion in thinner films.[7] The physical characterization of thin polymer films is notoriously difficult to obtain; single molecule probes offer a new approach to this long-standing problem.

A quick method for ascertaining the rotational mobility of an entire scan field of dye molecules on a surface or in a thin film[7] is demonstrated in Figure 5. As in normal sample scanning confocal microscopy, an image of the surface is acquired by scanning the sample through the focused laser spot. Here the polarization is modulated at 200 Hz while scanning, and the beginning of each scan line is synchronized with the start of a modulation sine wave. At each pixel, fluorescent photons are collected at the APD with 1 ms integration time. As a result of the polarization modulation of the excitation light, stationary molecules appear to have stripes across them with orientation perpendicular to the scan direction. The bright/dark regions

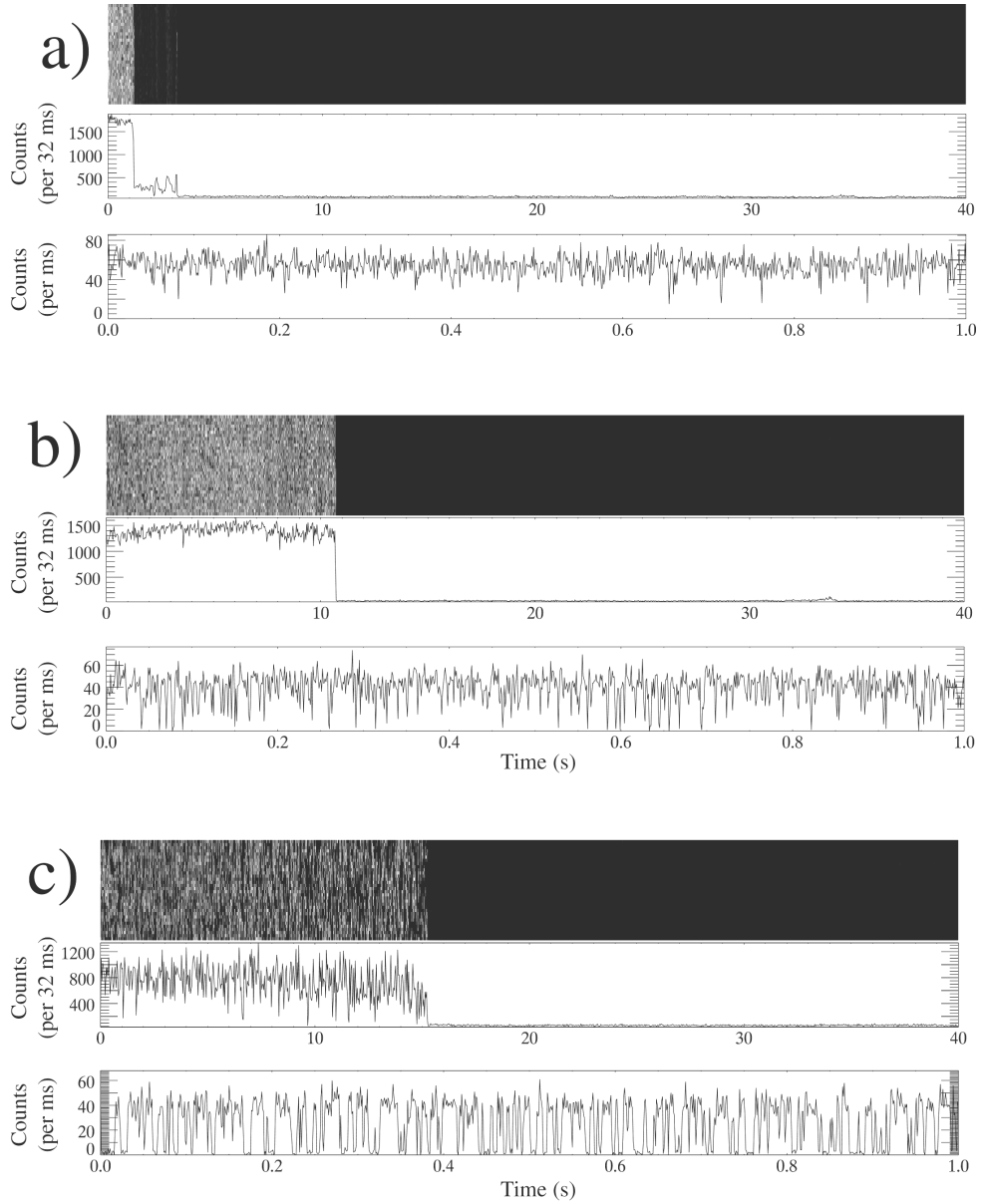

Figure 6. Representative intensity trajectories of single $DiIC_{18}$ molecules under O_2 purge (a), air purge (b), and N_2 purge (c) conditions. In each case, the molecules are embedded in a thin PS film and the data are acquired with 1 ms bins for 40 s. The data are plotted under each panel with 32 ms binning. In addition, expanded views of the first 1 s of data are shown for each.

correspond to times at which the polarization of the excitation light is parallel/perpendicular to the absorption dipole moment. Molecules that change orientation during the imaging process show a shift in the position of these stripes (the stripes are discontinuous and look ragged or broken). Figure 5 shows a 20 μm × 20 μm (600 pixels × 600 pixels) image produced using this method for $DiIC_{18}$ molecules in a 60 nm thick PVB film. The fast scan axis is vertical and the illumination power level was 1 μW. Note that this technique is also useful for distinguishing between single molecules which have a well-defined absorption dipole axis and clusters of molecules that have only partial or no sensitivity to the polarization of the excitation light. Here we can immediately pick out molecules with rotational mobility, and we can easily see that most of the molecules in this image are stationary.

2. MOLECULES IN DIFFERENT GASEOUS ENVIRONMENTS

So far we have discussed one way in which the molecular transition rates - in particular k_{abs} - can be affected by the local environment of the molecule. Since a direct radiative triplet to singlet transition is forbidden, the triplet lifetime τ_{T_1} will depend on molecular collisions, and in particular the presence of oxygen. Photobleaching also depends on oxygen concentration and is generally considered to be due to oxidation from the triplet state. Both of these phenomena are evident in Figure 6, where intensity vs. time is plotted for three molecules. These examples were selected from data sets taken on samples prepared identically, but acquired while purging with O_2 (Fig. 6a), in air (Fig. 6b), and while purging with N_2 (Fig. 6c). While a great range of behavior, similar to the molecule in Figure 1, can be observed for each experimental condition, on the average we see longer lifetime before photobleaching and longer τ_{T_1} as the oxygen content is decreased. Even though the DiC_{18} molecules are embedded in a thin (approximately 50 nm) polystyrene film, the effect of adjusting the oxygen content is significant. The same format as used in Figure 1 is used again in Figure 6; below the grayscale panel showing all the intensity data, the total number of photons counted in each 32 ms column is plotted. At about 4 s the molecule in Figure 6a photobleaches. Prior to photobleaching, there is only very weak evidence of a triplet state. The first second of data are shown in the bottom panel of Figure 6a. The average value of the count rate is 54.3 ms^{-1} and the rms noise is 9.97 ms^{-1} (compared to 7.4 ms^{-1} for a Poisson distribution). In other cases the intensity distribution in oxygen is perfectly Poisson and the triplet effect is undetected. In Figure 6b, in which the molecule is in room air, the downward spikes indicative of triplet shelving become evident and the distribution is very clearly not Poisson. In a nitrogen atmosphere, or in vacuum,[24] the triplet state is significantly lengthened and the triplet effects are apparent for a majority of molecules present. Figure 6c shows a single molecule in the same PS film under nitrogen atmosphere. Here the dark triplet state is clearly evident in the bottom, as the intensity repeatedly falls to the background for intervals over a millisecond. Without oxygen, the molecule also lives longer, photobleaching near 15 s. Again we point out that a wide variety of intensity fluctuation phenomena are observed for each experiment condition and the choices shown here were selected to demonstrate these basic trends that we have observed.

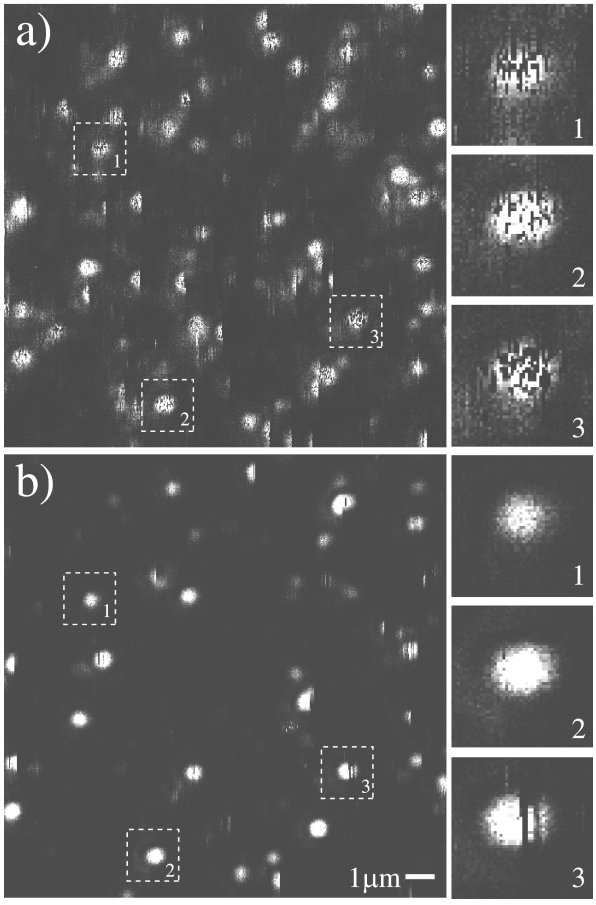

Figure 7. Images of the same scan field of view of $DiIC_{18}$ molecules under N_2 purge (a) and under O_2 purge (b). Expanded views of three different molecules under both conditions are shown in the panels to the right of each image.

The triplet state lifetime dependence on the presence of oxygen is demonstrated again in Figure 7 which shows confocal images of the same area of molecules while purging with N_2 (Fig. 7a) and while purging with O_2 (Fig. 7b). Expanded views of three different molecules (labeled 1, 2, and 3) are shown for both conditions. The "speckle" evident in the top image

(nitrogen) is not noise - rather it is the intermittency brought on by an extended τ_{T_1}. In Figure 7b, this effect almost completely disappears as τ_{T_1} decreases with oxygen content.

3. MOLECULES IN AQUEOUS BUFFER

3.1 In solution

Single molecule studies of biological molecules are generally done in aqueous solution, with the molecules either tethered to a surface or free to diffuse in the bulk. Ideally, we would like to study the interactions of biomolecules in their natural environment, *e.g.*, inside a cell or cell membrane. More and more, single molecule probes are being used in living organisms.[13-15] But when studying a molecule *in-vivo* is not possible, or when the goal is a high-throughput *in-vitro* screen or binding assay, it is often possible to detect and study single tagged molecules in solution. Indeed, the earliest single molecule detection schemes were in liquid, [45] including a proposed technique for DNA sequencing using fluorescence detection of single molecules.[46]

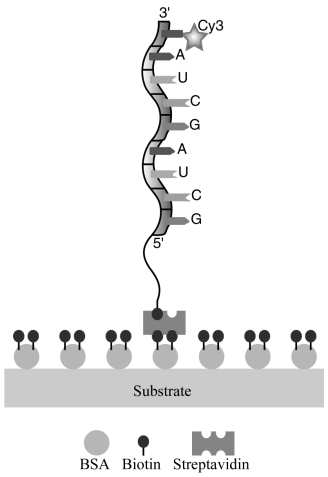

Figure 8. Tethering RNA to a surface.

When working in solution, with the molecule free to diffuse or flowing through the confocal detection volume, the detection time of any one molecule is limited to the time it spends in the confocal volume. For small molecules in aqueous solution this time can be a fraction of a millisecond. By observing many such events, one can measure diffusion coefficients, or determine concentrations of various diffusing species that may be present. A large body of literature exists on the use of fluorescence fluctuation correlation spectroscopy in this context.[47,48] Some applications of this technique are to sorting single molecules,[48] mapping the flow field in microchannels,[49] and detection of prion-protein aggregates.[50] If we want to watch the dynamics of a single molecule over time, for example to observe enzymatic turnovers or structural changes upon binding, we need a molecule that remains within the detection volume so we can observe its behavior for a longer duration, preferably for many seconds, or even hours. Schemes for immobilizing molecules without disrupting their normal activity have involved placing the molecule in an aqueous gel[19,51] or tethering the molecule to a surface.[20,52,53] Here we concentrate on the latter.

3.2 Bound to a surface

A number of recent single molecule experiments rely on the ability to tether a molecule without significantly changing its activity.[20,52,53] A common scheme for tethering nucleic acids to surfaces exploits the high affinity bond of biotin with streptavidin (dissociation constant $K_d \sim 10^{-15}$M) shown schematically in Figure 8. Here, a single stranded RNA molecule is labeled with Cy3™ (Amersham Pharmacia Biotech Ltd.) at its 3' end. At the 5' end, a single biotin molecule is attached to the RNA via a flexible tether. Streptavidin, which is a homo-tretramer, links the biotinylated RNA molecule to a coverslip coated with biotinylated bovine serum albumin (BSA).

If we use the scheme discussed above for measuring the rotational behavior of these molecules we find that the dynamics of the fluorophore are modified by the surface. In Figure 9 we show an image, taken the same way as the image in Figure 5, of these molecules. This sample is prepared by exposing a clean glass substrate to 1mg/ml biotinylated BSA, then 1mg/ml streptavidin, and finally 1 nmol/L RNA labeled as described above. The absence of stripes on many of these molecules indicates that those molecules are rotating freely. However, there are many molecules that show at least some

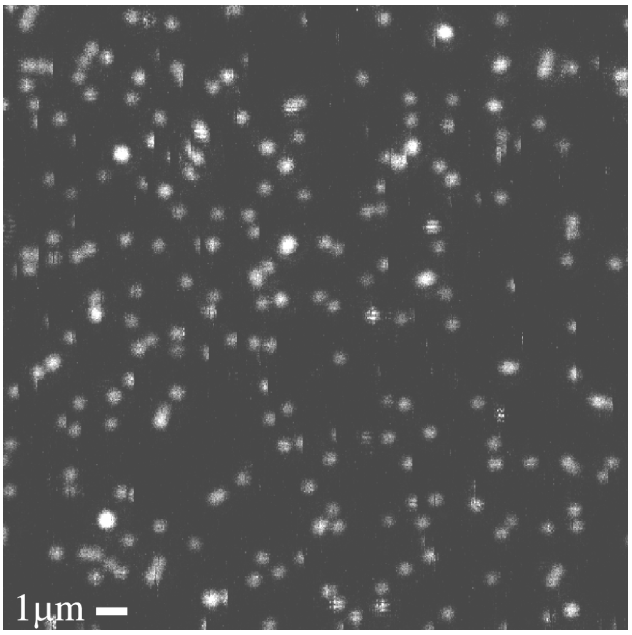

Figure 9. Single RNA molecules in aqueous buffer. The beginning of each scan line (vertical) is synchronized with the initiation of polarization rotation, as in Figure 5.

evidence of stripes, meaning that rotation in these cases is hindered. For these molecules, the rotational diffusion of the fluorophore, and probably also the rest of the molecule, is inhibited by the presence of the surface.

In Figure 10 we show the intensity fluctuation behavior and rotational dynamics of three selected examples of Cy3 tagged RNA surface tethered molecules. The data are acquired and displayed as in Figure 1, except that the total observation time per molecule is 6.4 s. We can see in Figure 10 that there are periods of time in which the fluorescence becomes modulated, indicating that there is a tendency for these molecules to stick to the surface. In addition, we see that there are associated

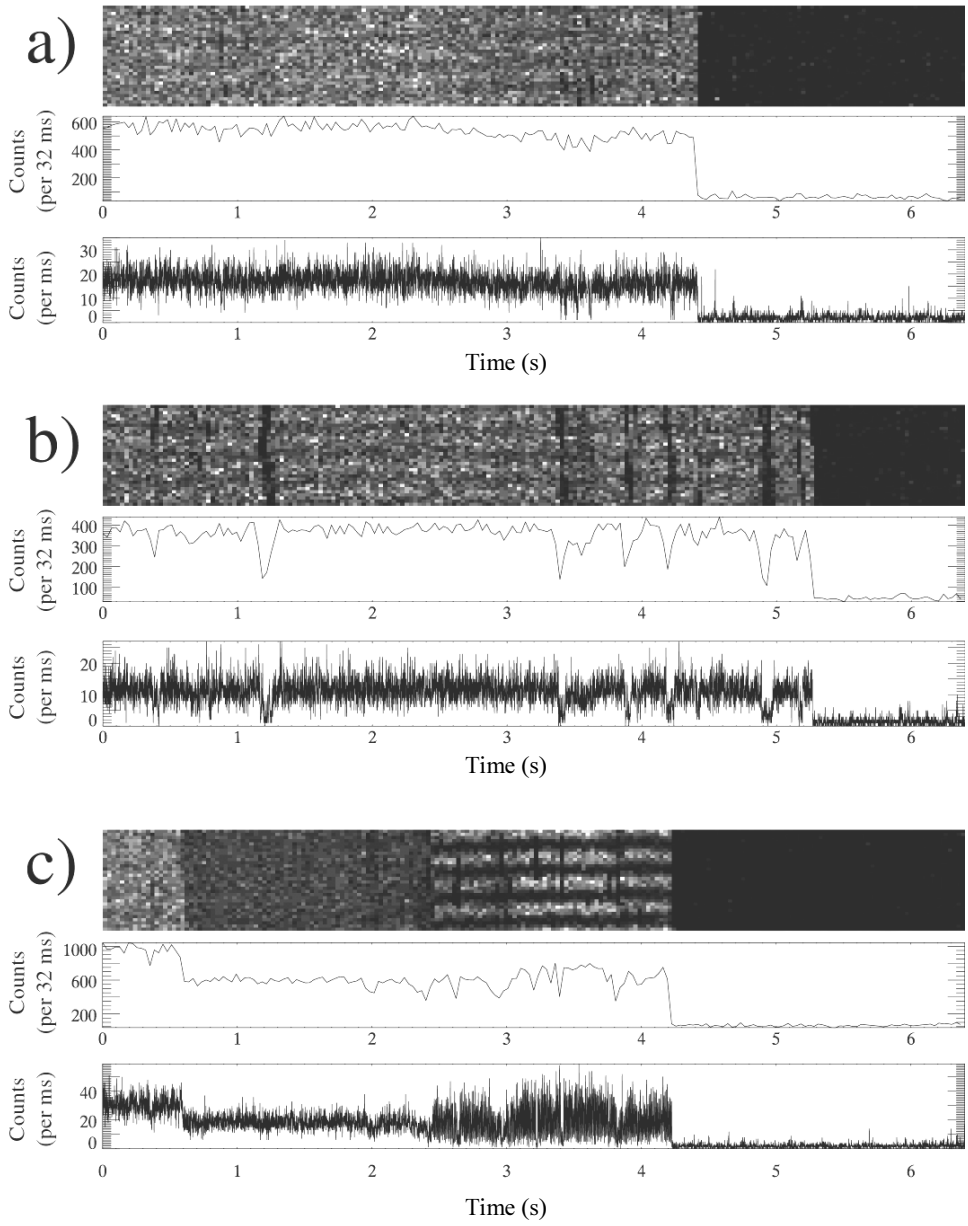

Figure 10. Representative intensity trajectories of single Cy3 molecules attached to RNA tethered to a surface, as described in the text. The excitation light is polarization modulated at 125 Hz. The data are plotted under each panel with 32 ms binning and with 1 ms binning. Striped regions indicate times when the rotation of the molecule was hindered by the surface.

intensity fluctuations in the fluorescence. Here the polarization modulation leads to intensity modulations that are evident as clear stripes at about 2.5 s to 4.0 s in Figure 10c. Weak stripes are in evidence elsewhere, indicating that these molecules are not perfectly free to rotate.

This hindered motion has implications in single molecule studies of RNA binding and folding. Frequently, fluorescence resonant energy transfer (FRET) or fluorescence quenching is used to determine intra- or inter-molecular distances or conformation. These techniques use changes in fluorescence intensity (via changes in k_{fl} or $k_{nr}^{S_1}$) to determine changes in distance in the 0.1 nm -10 nm range. The effect of rotational dynamics and intensity fluctuations are generally ignored in these studies. Intensity fluctuations due to triplet shelving might well be ignored for molecules in aqueous buffer, where triplet lifetimes tend to be short. However, for tethered molecules such as those shown here (where hindered motion of the fluorophore occurs) the effect of orientation on FRET or quenching needs to be considered. In the case of quenching, a fluorescent lifetime measurement might be more informative than a simple measurement of fluorescence intensity, since this probes k_{fl} directly and is not affected by changes in k_{abs} caused by rotation of the molecule. To the extent that the surface may also modify k_{fl}, we have a problem that is more difficult to solve.

Why are some of the molecules in Figure 9 apparently free to move and others hindered? Here, as in the polymer case, we have evidence for local heterogeneity of the surface. It may be possible that a careful study of this surface, and of surfaces prepared with different protocols, will result in a more effective substrate for tethered RNA assays.

ACKNOWLEDGMENTS

We are grateful to the NIST ATP intramural program for supporting our work on single molecule dynamics. Certain commercial equipment, instruments, or materials are identified in this paper to foster understanding. Such identification does not imply recommendations or endorsements by the National Institute of Standards and Technology, nor does it imply that the materials or equipment identified are necessarily the best available for the purpose.

REFERERNCES

1. Plakhotnik, T., Donley, E. A. & Wild, U. P. "Single-molecule spectroscopy," *Annu. Rev. Phys. Chem.* **48**, 181-212 (1997).
2. Xie, X. S. & Trautman, J. K. "Optical studies of single molecules at room temperature," *Annu. Rev. Phys. Chem.* **49**, 441-480 (1998).
3. Moerner, W. E. & Orrit, M. "Illuminating single molecules in condensed matter," *Science* **283**, 1670-1676 (1999).
4. Weiss, S. "Fluorescence spectroscopy of single biomolecules," *Science* **283**, 1676-1683 (1999).
5. Hou, Y. W., Bardo, A. M., Martinez, C. & Higgins, D. A. "Characterization of molecular scale environments in polymer films by single molecule spectroscopy," *J. Phys. Chem. B* **104**, 212-219 (2000).
6. Deschenes, L. A. a. V. B., D.A. "Single molecule studies of heterogeneous dynamics in polymer melts near the glass transition," *Science* **292**, 255-258 (2001).
7. Weston, K. D. & Goldner, L. S. "Orientation imaging and reorientation dynamics of single dye molecules," *J. Phys. Chem. B* **105**, 3453-3462 (2001).
8. Wang, H. M., Bardo, A. M., Collinson, M. M. & Higgins, D. A. "Microheterogeneity in dye-doped silicate and polymer films," *J. Phys. Chem. B* **102**, 7231-7237 (1998).
9. Mei, E., Bardo, A. M., Collinson, M. M. & Higgins, D. A. "Single-molecule studies of sol-gel-derived silicate films. Microenvironments and film-drying conditions," *J. Phys. Chem. B* **104**, 9973-9980 (2000).
10. Talley, C. E. & Dunn, R. C. "Single molecules as probes of lipid membrane microenvironments," *J. Phys. Chem. B* **103**, 10214-10220 (1999).
11. Hollars, C. W. & Dunn, R. C. "Probing single molecule orientations in model lipid membranes with near-field scanning optical microscopy," *J. Chem. Phys.* **112**, 7822-7830 (2000).
12. Sonnleitner, A., Schutz, G. J. & Schmidt, T. "Free Brownian motion of individual lipid molecules in biomembranes," *Biophys. J.* **77**, 2638-2642 (1999).
13. Sako, Y., Minoghchi, S. & Yanagida, T. "Single-molecule imaging of EGFR signalling on the surface of living cells," *Nat. Cell Biol.* **2**, 168-172 (2000).
14. Byassee, T. A., Chan, W. C. W. & Nie, S. M. "Probing single molecules in single living cells," *Anal. Chem.* **72**, 5606-5611 (2000).
15. Schutz, G. J., Pastushenko, V.Ph.,Gruber, H.J., Knaus, H.-G., Pragl, B, and Schindler, H. "3D Imaging of Individual Ion Channels in Live Cells at 40 nm Resolution," *Single Molecules* **1**, 25-31 (2000).
16. Vale, R. D. et al. "Direct observation of single kinesin molecules moving along microtubules," *Nature* **380**, 451-453 (1996).
17. Sase, I., Miyata, H., Ishiwata, S. & Kinosita, K. "Axial rotation of sliding actin filaments revealed by single- fluorophore imaging," *Proc. Natl. Acad. Sci. U. S. A.* **94**, 5646-5650 (1997).
18. Warshaw, D. M. et al. "Myosin conformational states determined by single fluorophore polarization," *Proc. Natl. Acad. Sci. U. S. A.* **95**, 8034-8039 (1998).
19. Lu, H. P., Xun, L. Y. & Xie, X. S. "Single-molecule enzymatic dynamics," *Science* **282**, 1877-1882 (1998).
20. Ha, T. J. et al. "Single-molecule fluorescence spectroscopy of enzyme conformational dynamics and cleavage mechanism," *Proc. Natl. Acad. Sci. U. S. A.* **96**, 893-898 (1999).
21. Zhuang, X. W. et al. "Fluorescence quenching: A tool for single-molecule protein- folding study," *Proc. Natl. Acad. Sci. U. S. A.* **97**, 14241-14244 (2000).

22. Bopp, M. A., Sytnik, A., Howard, T. D., Cogdell, R. J. & Hochstrasser, R. M. "The dynamics of structural deformations of immobilized single light-harvesting complexes," *Proc. Natl. Acad. Sci. U. S. A.* **96**, 11271-11276 (1999).
23. Ha, T., Enderle, T., Chemla, D. S., Selvin, P. R. & Weiss, S. "Quantum jumps of single molecules at room temperature," *Chem. Phys. Lett.* **271**, 1-5 (1997).
24. Weston, K. D., Carson, P. J., DeAro, J. A. & Buratto, S. K. "Single-molecule detection fluorescence of surface-bound species in vacuum," *Chem. Phys. Lett.* **308**, 58-64 (1999).
25. English, D. S., Furube, A. & Barbara, P. F. "Single-molecule spectroscopy in oxygen-depleted polymer films," *Chem. Phys. Lett.* **324**, 15-19 (2000).
26. Veerman, J. A., Garcia-Parajo, M. F., Kuipers, L. & van Hulst, N. F. "Time-varying triplet state lifetimes of single molecules," *Phys. Rev. Lett.* **83**, 2155-2158 (1999).
27. Weston, K. D., Carson, P. J., Metiu, H. & Buratto, S. K. "Room-temperature fluorescence characteristics of single dye molecules adsorbed on a glass surface," *J. Chem. Phys.* **109**, 7474-7485 (1998).
28. Weston, K. D. & Buratto, S. K. "Millisecond intensity fluctuations of single molecules at room temperature," *J. Phys. Chem. A* **102**, 3635-3638 (1998).
29. Higgins, D. A., VandenBout, D. A., Kerimo, J. & Barbara, P. F. "Polarization-modulation near-field scanning optical microscopy of mesostructured materials," *J. Phys. Chem.* **100**, 13794-13803 (1996).
30. Ha, T., Enderle, T., Chemla, D. S., Selvin, P. R. & Weiss, S. "Single molecule dynamics studied by polarization modulation," *Phys. Rev. Lett.* **77**, 3979-3982 (1996).
31. Dickson, R. M., Norris, D. J. & Moerner, W. E. "Simultaneous imaging of individual molecules aligned both parallel and perpendicular to the optic axis," *Phys. Rev. Lett.* **81**, 5322-5325 (1998).
32. Jasny, J. & Sepiol, J. "Single molecules observed by immersion mirror objective. A novel method of finding the orientation of a radiating dipole," *Chem. Phys. Lett.* **273**, 439-443 (1997).
33. Bopp, M. A., Jia, Y., Haran, G., Morlino, E. A. & Hochstrasser, R. M. "Single-molecule spectroscopy with 27 fs pulses: Time-resolved experiments and direct imaging of orientational distributions," *Appl. Phys. Lett.* **73**, 7-9 (1998).
34. Fourkas, J. T. "Rapid determination of the three-dimensional orientation of single molecules," *Opt. Lett.* **26**, 211-213 (2001).
35. Tanaka, H., Ishijima, A., Honda, M., Saito, K. & Yanagida, T. "Orientation dependence of displacements by a single one-headed myosin relative to the actin filament," *Biophys. J.* **75**, 1886-1894 (1998).
36. Ha, T. et al. "Probing the interaction between two single molecules: Fluorescence resonance energy transfer between a single donor and a single acceptor," *Proc. Natl. Acad. Sci. U. S. A.* **93**, 6264-6268 (1996).
37. Ha, T. J. et al. "Temporal fluctuations of fluorescence resonance energy transfer between two dyes conjugated to a single protein," *Chem. Phys.* **247**, 107-118 (1999).
38. Dhinojwala, A., Wong, G. K. & Torkelson, J. M. "Rotational Reorientation Dynamics of Disperse Red-1 in Polystyrene - Alpha-Relaxation Dynamics Probed By 2nd-Harmonic Generation and Dielectric-Relaxation," *J. Chem. Phys.* **100**, 6046-6054 (1994).
39. Hampsch, H. L., Yang, J., Wong, G. K. & Torkelson, J. M. "Dopant Orientation Dynamics in Doped 2nd-Order Nonlinear Optical Amorphous Polymers .2. Effects of Physical Aging On Poled Films," *Macromolecules* **23**, 3648-3654 (1990).
40. Hall, D. B., Miller, R. D. & Torkelson, J. M. "Molecular probe techniques for studying diffusion and relaxation in thin and ultrathin polymer films," *J. Polym. Sci. Pt. B-Polym. Phys.* **35**, 2795-2802 (1997).
41. Mounir, E. S. A., Takahara, A. & Kajiyama, T. "Effect of chain end group-substrate interaction on surface molecular motion of polystyrene ultrathin films," *Polym. J.* **31**, 550-556 (1999).
42. DeMaggio, G. B. et al. "Interface and surface effects on the glass transition in thin polystyrene films," *Phys. Rev. Lett.* **78**, 1524-1527 (1997).
43. Tanaka, K., Taura, A., Ge, S. R., Takahara, A. & Kajiyama, T. "Molecular weight dependence of surface dynamic viscoelastic properties for the monodisperse polystyrene film," *Macromolecules* **29**, 3040-3042 (1996).
44. According to ISO 31-8, the term "molecular weight" has been replaced with the "relative molecular mass," symbol *Mr*. The conventional notation, rather than the ISO notation, has been employed for this publication.
45. Dovichi, N. J., Martin, J. C., Jett, J. H., Trkula, M. & Keller, R. A. "Laser-Induced Fluorescence of Flowing Samples as an Approach to Single-Molecule Detection in Liquids," *Anal. Chem.* **56**, 348-354 (1984).
46. Jett, J. H. et al. "High-Speed Dna Sequencing - an Approach Based Upon Fluorescence Detection of Single Molecules," *J. Biomol. Struct. Dyn.* **7**, 301-309 (1989).
47. Qian, H. & Elson, E. L. "Analysis of Confocal Laser-Microscope Optics for 3-D Fluorescence Correlation Spectroscopy," *Appl. Optics* **30**, 1185-1195 (1991).
48. Eigen, M. & Rigler, R. "Sorting Single Molecules - Application to Diagnostics and Evolutionary Biotechnology," *Proc. Natl. Acad. Sci. U. S. A.* **91**, 5740-5747 (1994).
49. Gosch, M., Blom, H., Holm, J., Heino, T. & Rigler, R. "Hydrodynamic flow profiling in microchannel structures by single molecule fluorescence correlation spectroscopy," *Anal. Chem.* **72**, 3260-3265 (2000).
50. Bieschke, J. et al. "Ultrasensitive detection of pathological prion protein aggregates by dual-color scanning for intensely fluorescent targets," *Proc. Natl. Acad. Sci. U. S. A.* **97**, 5468-5473 (2000).
51. Dickson, R. M., Cubitt, A. B., Tsien, R. Y. & Moerner, W. E. "On/off blinking and switching behaviour of single molecules of green fluorescent protein," *Nature* **388**, 355-358 (1997).
52. Ha, T. et al. "Ligand-induced conformational changes observed in single RNA molecules," *Proc. Natl. Acad. Sci. U. S. A.* **96**, 9077-9082 (1999).
53. Zhuang, X. W. et al. "A single-molecule study of RNA catalysis and folding," *Science* **288**, 2048-2051 (2000).